Application of Poly-γ-Glutamic Acid Flocculant to Flocculation–Sedimentation Treatment of Ultrafine Cement Suspension

Tomokazu Yanagibashi [1],*, Motoyoshi Kobayashi [2] and Keisuke Omori [3]

[1]   Penta-Ocean Institute of Technology, 1534-1, Yonkucho, Nasushiobara, Tochigi 329-2746, Japan
[2]   Faculty of Life and Environmental Sciences, University of Tsukuba, 1-1-1, Tennodai, Tsukuba, Ibaraki 305-8572, Japan
[3]   Japan International Research Center for Agricultural Sciences, 1-1, Ohwashi, Tsukuba, Ibaraki 305-8686, Japan
*   Correspondence: tomokazu.yanagibashi@mail.penta-ocean.co.jp; Tel.: +81-(0)287-39-2116

Abstract: We examined the effect of poly-γ-glutamic acid flocculant (PGAF) on the removal of ultrafine cement (UFC) particles stabilized by a poly-carboxylate co-polymer, which is a superplasticizer (SP). The flocculation–sedimentation treatment with PGAF successfully removed the SP-stabilized cement particles through the gravitational settling of the formed flocs. The removal efficiency reduced with the increase in the ionic strength, probably because of the shrunk form of poly-γ-glutamic acid (γ-PGA) at high ionic strengths. Increasing the mixing intensity during rapid mixing improved the removal efficiency. A series of flocculation–sedimentation experiments provided a diagram showing the relationship between ionic strengths and the addition amount of PGAF. Our results suggest that PGAF is a good candidate for the purification of cement suspension by flocculation–sedimentation, and a better removal performance can be obtained at lower ionic strengths with intense rapid mixing. From the diagram of the control charts presented in this study, we can determine the optimal addition amount of PGAF for achieving the target removal rate for cement suspension under any ionic strength.

Keywords: flocculation; sedimentation; cement suspension; poly-γ-glutamic acid flocculant; superplasticizer; ionic strength; zeta potential

1. Introduction

The wastewater generated during construction work contains clay, sand, and cement. In particular, the wastewater generated during concrete casting or grouting contains suspended particles resulting from cement and chemical mixtures. In addition to suspended particles, such wastewaters contain various dissolved ions originating from cement hydration and thus show a high pH. Furthermore, as raw cement particles strongly agglomerate in water, cement suspensions have high viscosity and settling cement flocs. To avoid cement aggregation, a chemical admixture called superplasticizer (SP), which is a polymeric dispersant, is added to cement suspensions. These cause problems in the treatment of conventional cement wastewater: optimization of treatment facility design "on site" aggregation inhibition by coexisting substances (such as SP and various salts), and neutralization that reduces pH. In recent years, with the progress of material development, such as refinement of cement particles, use of chemical modifiers for cement surfaces, and composite materials with various admixtures, wastewater properties have significantly changed [1].

In the flocculation process performed in wastewater treatments, coagulants, flocculants, and coagulation aids are used to remove the electrostatic repulsion between particles and to enlarge the flocs. Hydrate polymers of aluminum, such as poly-aluminum chloride (PAC), are frequently used at

construction sites. These aluminum salts cause charge neutralization with aluminum ions and sweep flocculation with the precipitates of aluminum [2]. These flocculants exhibit a high performance in the neutral pH region, while the hydrolysis products are negatively charged. The removal performance is reduced at high pH. Therefore, to improve the performance of aluminum flocculants, it is necessary to adjust the pH to an appropriate range beforehand. This shows that PAC is not suitable for cement suspensions.

A recent study showed that the aluminum that remains in drinking water causes neuro-degenerative diseases in humans [3]. As such, the alternative use of natural organic coagulants derived from plants, such as *Moringa oleifera*, has attracted much interest. Several authors have studied the use of *Moringa oleifera* in water treatment in recent years [3,4]. De Paula et al. [4] reported the treatment of cement concrete wastewater by combining $Al_2(SO_4)_3$ and *Moringa oleifera*. They collected wastewater samples from the wastewater treatment system of an actual concrete plant and showed that 99% of the turbidity can be removed at a proposed ratio of $Al_2(SO_4)_3$ and *Moringa oleifera*. On the other hand, PGAF, which is also a type of natural organic flocculant, has attracted attention as a flocculant with a high flocculating effect [5–11]. However, studies on its removal performance for cement suspensions are lacking.

To determine the optimum conditions for a flocculation process, it is important to consider the removal characteristics in terms of the flocculation–sedimentation and charge characteristics of the particles in the mixed system. Accordingly, Kobayashi et al. [12] described coagulation and dispersion mechanisms, charge neutralization, and sweep coagulation in terms of the charging and coagulation properties of natural imogolite clay by conducting coagulation–sedimentation experiments in latex–imogolite mixed systems under various pH values. However, it is difficult to apply this method for cement suspensions obtained from construction sites, because the wastewaters generated at construction sites differ considerably depending on the type, method, and natural conditions. Furthermore, in the case of cement suspensions, the surface of the fine particles is usually modified by a chemical admixture, the ion species and concentration in the solvent are extremely complex, and the state of the fine particle surface changes as hydration progresses. Therefore, it is important to apply a flocculant for a well-controlled model cement suspension.

In this context, we aimed to investigate the applicability and removal characteristics of poly-γ-glutamic acid flocculant (PGAF) for model cement suspensions. To this end, we first measured the ion species dissolved in a cement suspension and their concentration. Second, based on the measured results of the dissolved ions, we established a method for preparing a model cement suspension under controlled cement concentration and ionic strength. Third, the coagulation–flocculation mechanisms and charge characteristics in the model systems were investigated, in which PGAF flocculants were added to the cement suspension under controlled ionic strength and cement concentration. Finally, based on the results, we discussed the removal mechanism and the applicability of this flocculant to cement suspensions.

2. Materials and Methods

2.1. Materials

2.1.1. Ultrafine Cement

For the experiments conducted in this study, we used ultrafine cement (UFC) (HNP-1500, Nippon Steel Sumikin Cement Co., Ltd., Tokyo, Japan), which is used as an injection material for waterproofing or reinforcement in tunnels and grounds. Figure 1a shows the particle size distributions of the UFC, ordinary Portland cement (OPC), and blast furnace slag cement (BFSC) particles measured using static image analysis (Morphologi 4, Malvern Panalytical, Malvern, UK). The removal characteristics of the UFC particles from the suspension were considered in this study. The OPC contained a considerable number of small particles with a size of approximately 1 μm; however, the particle size distribution was wide, making it difficult to prepare a model suspension. The UFC particles had an average particle

size of approximately 1.5 μm, and the particle size distribution was narrow. The raw material of UFC was mainly blast furnace slag, which has a low hydration activity, and the cement part contained a low content of $3CaO \cdot Al_2O_3$ with a rapid hydration reaction.
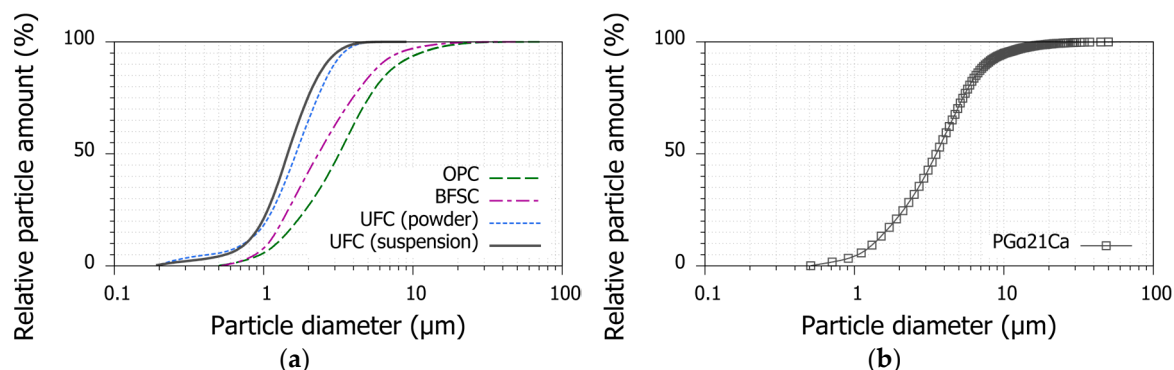

Figure 1. Cumulative number-based size distribution: (**a**) cements; (**b**) PGα21Ca as poly-γ-glutamic acid flocculant (PGAF). The ultrafine cement suspension contained 20 wt% superplasticizer solution (12.2 wt% polymer) based on cement mass. The other materials were measured under powdered conditions.

2.1.2. Polymeric Dispersant

A high-performance water-reducing agent (VP-700, FLOWRIC Co., Ltd., Tokyo, Japan) with a high dispersibility to cement particles was used as the SP for the UFC. Figure 2a shows the presumed chemical structure of the SP. UFC (HNP-1500) is recommended to be used as an injection material with a special dispersant as a high-performance air-entrainment (AE) water-reducing agent. In this study, however, a non-AE type of water-reducing agent was used to minimize the influence of entrained air on the aggregation and flocculation mechanisms. The cement suspensions with and without SP were compared by a microscope as shown in Figure 2b,c, and the monodispersity of UFC particles with SP was confirmed. The main component of this polycarboxylate ether-based SP is characterized by a backbone unit with carboxylic acid groups attached to the cement particles and a hydrophilic polyethylene oxide that induces a steric repulsive interparticle force, thus avoiding the formation of agglomerates as the side chain [13,14]. Although numerous studies have investigated the dispersing role of such SPs [13–16], their fundamental interaction mechanisms remain unclear.
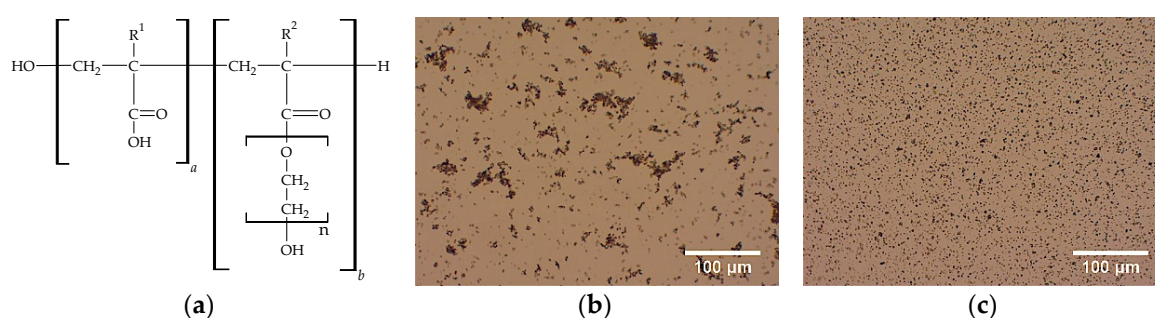

Figure 2. (**a**) Presumed chemical structure of the superplasticizer (SP); (**b**) micrograph of coagulated cement suspension with no SP; (**c**) micrograph of dispersed cement suspension with SP. The cement suspension concentration was 500 mg/L, and the amount of SP solution added was 20% with respect to the cement mass.

2.1.3. Flocculant

A food-derived amino acid-based polymer, namely the PGAF (PGα21Ca, Japan Poly-Glu Co., Ltd., Osaka, Japan), was used as the flocculant. Figure 3 shows the appearance of PGα21Ca. PGα21Ca is a natural polymer consisting of γ-PGA, which is an amino acid obtained from *Bacillus subtilis* [7].

PGα21Ca is composed of cross-linked γ-PGA with an average molecular weight of 10^7 and natural minerals such as calcium sulfate and calcium carbonate hydrate. The particle size of these minerals in dry powder (d_{50} = 3.49 μm) is greater than that of UFC particles, as shown in Figure 1b. As these minerals are known to promote coagulation through charge neutralization, they can aggregate even when added to pure water, as shown in Figure 3b. These characteristics make handling easier, allowing direct addition of PGα21Ca powder into water even when treating a small amount of wastewater. PGα21Ca can be applied at a wide range of pH and is expected to be effective against high-pH cement suspensions. However, studies on the application of PGα21Ca to cement wastewater and experimental results unveiling the aggregation mechanism are lacking. There are no technical guidelines for the appropriate use of PGα21Ca as PGAF.
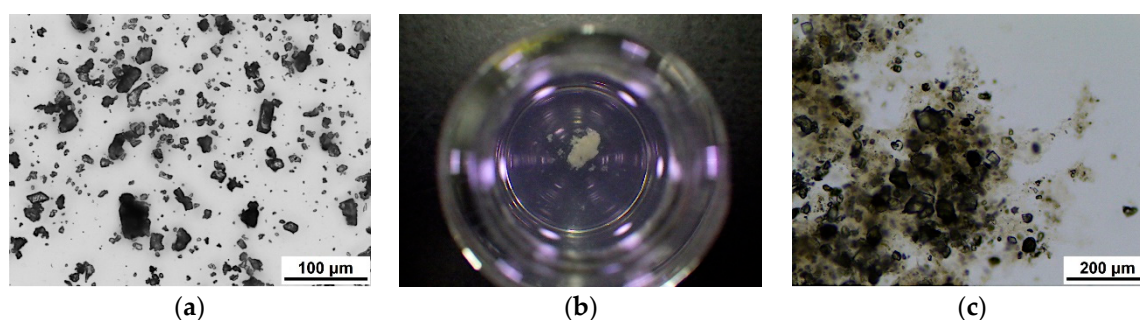

(a)   (b)   (c)

Figure 3. Images of PGα21Ca: (**a**) micrograph of dry powder; (**b**) precipitates after being added in pure water; (**c**) micrograph of precipitates in pure water. Clearly, PGα21Ca has the property to flocculate itself in pure water and enmesh its own mineral substances.

2.2. Cement Suspension

A predetermined mass of UFC particles (Table 1) was added to 1 L of pure water to prepare cement suspensions of various concentrations. After the cement addition, the cement suspension was stirred at a high speed for 1 min using a household mixer (IHB-602-W, IRIS OHYAMA, Miyagi, Japan). The suspension was then transferred to a polypropylene bottle and sonicated for 5 min (VS-D100, AS ONE Corporation, Osaka, Japan) while mixing with a glass rod. The bottle was then placed on a shaker operating at 150 rpm (MMS-2000, EYERA, Tokyo, Japan). After 3 h, the supernatant was collected and filtered using a syringe filter (0.45 μm). The filtrate was diluted to ensure that the electrical conductivity (EC) was less than 100 μS/cm, and the ion concentration was measured using ion chromatography (Prominence HIP-SP, SHIMADZU, Kyoto, Japan). In addition, the pH (LAQUA D-74, Horiba, Kyoto, Japan) and EC (LAQUAtwin EC-33, Horiba) of the filtrate were measured.

Table 1. Measurement items.

Cement Concentration	0.5, 1, 2, 10, and 100 (g/L)
Measurement items	Na$^+$, K$^+$, Ca^{2+}, Cl$^-$, SO$_4{}^{2-}$, pH, EC

The ionic composition and concentration of the pore water in cement pastes vary depending on the cement type and extraction pressure [17,18]. In this experiment, Na$^+$, K$^+$, Ca^{2+}, Cl$^-$, and SO$_4{}^{2-}$ were measured as main ions based on the results [19–21] of the bulk concentration of the cement suspension. The ionic strength of the bulk solution I_c can be calculated from the measured molar concentration of the ions m_i and the ionic valence z_i, as follows.

$$I_c = \frac{1}{2} \sum_i m_i z_i{}^2 = \frac{1}{2}\left(m_{\text{Na}^+} + m_{\text{K}^+} + 4m_{\text{Ca}^{2+}} + m_{\text{OH}^-} + 4m_{\text{SO}_4{}^{2-}} + m_{\text{Cl}^-}\right). \tag{1}$$

2.3. Flocculation–Sedimentation Experiments

2.3.1. Preparation of Ultrafine Cement Suspension

The concentration of UFC suspension (C_0) for the jar test was set to 500 mg/L with different ionic strengths by mixing the same volume of the cement suspension and extracted solutions from the cement suspension. The water-to-cement mass ratios (w/c) were 1000 in the suspension and 10, 100, 500, 1000, and 2000 for extracting the salt solutions for dilution. The extracted solutions from the cement suspension were prepared using the same procedure as that for the measurement of the ion concentration described above: a predetermined mass of UFC was added to 1 L of pure water and stirred at a high speed for 1 min using a household mixer. The suspension was transferred to a polypropylene bottle and sonicated for 5 min while mixing using a glass rod. The polypropylene bottle was set on a shaker and agitated at 150 rpm. After 3 h, the solution filtered through a 0.45 μm filter was used as an extraction solution in the experiment. In the case of the cement suspension, the SP was dissolved in pure water before the cement was added to the pure water. The ionic strength varies with the w/c. Thus, we prepared 500 mg/L cement suspensions with various ionic strengths by mixing the cement suspension and the extracted solution based on different w/c values. The pure water used in this study was distilled water (WA570, Yamato Scientific Co., Ltd., Tokyo, Japan).

2.3.2. Jar Test Procedure

The flocculation–sedimentation experiments were conducted using jar tester equipment (JMD-2E, Miyamoto Riken Ind. Co., Ltd., Osaka, Japan) at room temperature (20 °C). The width of the blade was 50 mm, and its height was 16 mm. We poured 300 mL of the UFC suspension prepared above into a tall beaker and added a predetermined mass of the PGAF. After the tall beaker was placed in the jar test equipment, the experiment was started. The experiments were conducted in three sequential steps: (1) rapid mixing at 150 rpm for 3 min; (2) slow mixing at 40 rpm for 10 min, and (3) settling for 30 min without mixing. After this sequence, 4 mL of the supernatant was collected to avoid surface floss, and the absorbance (C) at 660 nm was measured using a spectrophotometer (U-5100, Hitachi High-Technologies Corporation, Tokyo, Japan). The absorbance was proportional to the UFC concentration. Moreover, to investigate the influence of the mixing intensity, another experiment, in which step (1) of the above procedure was changed to step rapid mixing at 240 rpm for 5 min with double blade, was conducted.

Figure 4 shows the energy input rate calculated from the relationship between the torque measured using a mechanical torque meter (5TM1MN, Tohnichi Manufacturing Co., Ltd., Tokyo, Japan) and the rotational speed. The energy input rate per unit mass ε was 1.31×10^{-2} m^2/s^3 at 150 rpm and 5.12×10^{-2} m^2/s^3 at 240 rpm for the two blades. These correspond to G-values $(\varepsilon/\nu)^{1/2}$ of 114 and 224 s^{-1}, respectively [22].

The ionic strength is expected to have a significant effect on the flocculation process of the SP-stabilized UFC by PGAF. To analyze the flocculation process in more detail, we observed the structure of flocs formed under high and low ionic strengths using a microscope. For an ionic strength (I_C) = 5.4 mM and a PGAF-to-UFC mass ratio (m_f/m_c) of 0.2 (Case a) and for an I_C of 15.5 mM and a m_f/m_c of 0.2 (Case b), the flocs formed in the upper part at the end of rapid mixing were collected, and their shapes were compared in terms of the particle size distribution, circularity, and aspect ratio measured by static image analysis.
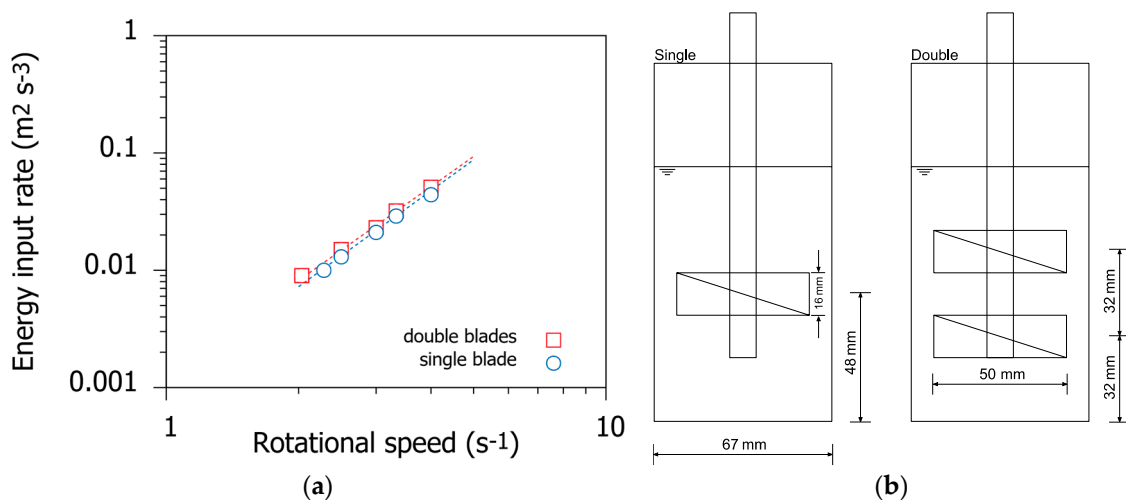
Figure 4. (**a**) Relationship between the rotational speed and the energy input rate per unit mass for different numbers of stirring blades. The energy input rate ε_i was determined using $\varepsilon_i = 2\pi N_r T_r / \rho V$, where N_r is the number of rotations per second, T_r is the torque, ρ and V are the density and volume of the medium, respectively; (**b**) front diagram of the stirring vessel and stirring blade.

2.3.3. Measurement of Zeta Potential

The electro–kinetic behavior of the particles gives a valuable indication of their surface charge state. Knowing the charge state in a system leads to a deeper understanding of the particle–particle interaction and thus aggregation and dispersion mechanisms. Therefore, we obtained the zeta potentials of the UFC, PGAF, and supernatant of these mixtures after sedimentation at various ionic strengths.

The zeta potential is highly sensitive to the chemical composition of the solvent such as ionic species, pH, and conductivity [23,24]. Many zeta potential measurements have been performed on cement particles [19–21,25–31]; measurements have been performed on OPCs, BFSCs [19,21,26,31], hydrated materials [20,25,28,29], and minerals for admixture [27,30]. Nevertheless, the data for UFC used in this study were not reported. In addition, there are some cases wherein SPs were added to the system [28–31]; however, these were measured using an electroacoustic method in high-concentration systems [28–30] or different conditions of solution even in the case of diluted systems [31]. Therefore, it was necessary to measure the zeta potential under the conditions established in this experiment. The coagulation experiments were carried out in the same manner as the jar test. After settling for 120 min, 10 mL of the supernatant was collected. The electrophoretic mobility μ was measured using a Zetasizer Nano ZS (Malvern Panalytical, Ltd., Malvern, UK). The average diameter of the UFC used in this study was approximately 1.5 μm; thus, the electrical double layer was considered thin enough. Therefore, the zeta potential ζ could be calculated using the following Smoluchowski's expression,

$$\mu = \frac{\varepsilon_r \varepsilon_0}{\eta} \zeta \tag{2}$$

where, ε_r is the relative dielectric constant of the liquid medium, ε_0 is the dielectric permittivity of vacuum, and η is the viscosity of the liquid medium. In water at 20 °C, $\varepsilon_r = 80$ and $\eta = 1.005$ mPa·s.

In addition, the electrophoretic mobilities of UFC and PGAF were measured as a function of the ionic strength using the method described above. The cement suspension was prepared by mixing the cement suspension with w/c = 2000 and various extracted solutions with different ionic strengths at a ratio of 1 to 9. On the other hand, the PGAF suspension was prepared by adding 8 mg of PGAF to 8 mL of the cement extracted solutions. Each sample was dispersed by ultra-sonication for 5 min and allowed to stand for 120 min before the measurement.

3. Results and Discussion

3.1. Ionic Composition of Cement Extract Solutions

Table 2 lists the ionic concentrations of the cement extract solutions measured by ion chromatography and the ionic strengths calculated from the measured data. As expected, the concentration of each ion species increased with the increase in the cement concentration, i.e., with the decrease in the w/c. The concentrations of calcium and hydroxide ions contributed approximately 80% to the ionic strength. The Debye length, which is an index of the thickness of the diffuse double layer, was calculated from the obtained ionic strength. The maximum Debye length was 4.94 nm, which was sufficiently lower than the particle diameter (1.5 μm).

Table 2. Ionic concentrations (mM) determined by ion chromatography, and ionic strengths calculated from the measured data for ultrafine cement (UFC) in pure water.

	Items	100 g/L (w/c = 10)	10 g/L (w/c = 100)	2 g/L (w/c = 500)	1 g/L (w/c = 1000)	0.5 g/L (w/c = 2000)
Data of ion chromatography	Na^+	3.65	0.23	0.14	0.21	0.28
	K^+	2.39	0.27	0.13	0.04	0.00
	Ca^{2+}	21.80	6.09	4.44	2.10	1.28
	Cl^-	0.73	0.08	0.04	0.01	0.00
	SO_4^{2-}	9.47	1.52	0.90	0.34	0.12
Data of pH	pH	12.51	12.23	11.66	11.46	11.27
	OH^-	32.36	16.98	4.57	2.88	1.86
Calculations	I_C	82.11	24.00	13.12	6.45	3.87
	$1/\kappa$ (nm) [1]	1.07	1.98	2.68	3.83	4.94

[1] The thickness of the diffuse layer can be determined using $\kappa = \sqrt{2N_A e^2 I_c / \varepsilon_r \varepsilon_0 kT}$; where κ is the Debye–Huckel parameter, e is the elementary charge, N_A is the Avogadro's number, and k is the Boltzmann's constant.

3.2. Particle Removal by Poly-γ-Glutamic Acid Flocculant (PGAF)

Figure 5a shows the ratio of the absorbance of the supernatant to that of the initial suspension (C/C_0) plotted against the m_f/m_c at different ionic strengths. A reduction in C/C_0 implies the removal of particles, whereas $C/C_0 = 1$ for no-removal. The figure shows that PGAF had a particle removal ability through flocculation–sedimentation for cement suspensions even under severe conditions of high pH.
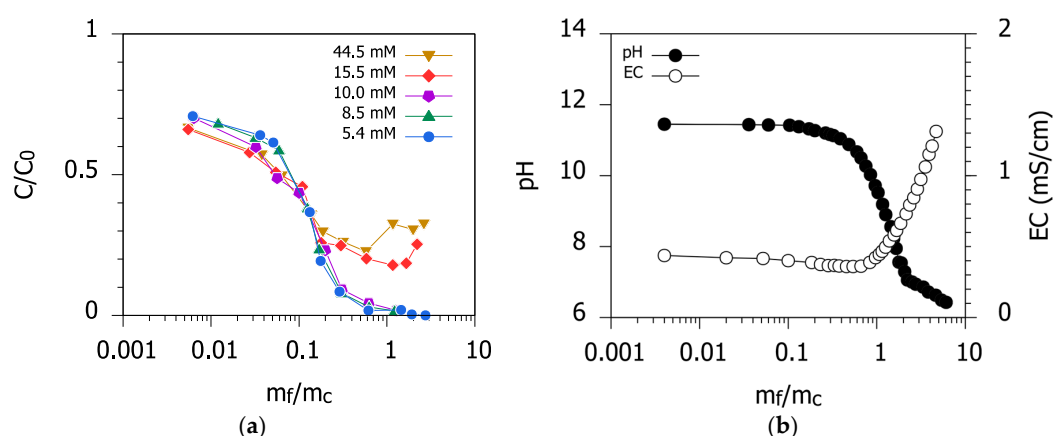

Figure 5. (**a**) Variation in the absorbance relative to the initial absorbance (C/C_0) with respect to the PGAF-to-UFC mass ratio (m_f/m_c) at each ionic strength; (**b**) variations in pH and electrical conductivity (EC) with respect to the m_f/m_c in the cement suspension of ionic strength (I_C) = 5.4 mM.

The concentration of the cement suspension was set to a somewhat high value of 500 mg/L. Thus, the PGAF dose was more than the value (50–100 mg/L) recommended by the manufacturer. For cement suspensions with I_C in the range of 5.4–10 mM, the C/C_0 value was reduced to 0.1 or less

when $m_f/m_C = 0.3$. For cement suspensions with $I_C = 15.5$ and 44.5 mM, C/C_0 was slightly lower than that when I_C was in the range of 5.4–10 mM when m_f/m_c was lower than 0.1. Once m_f/m_c exceeded 0.1, the C/C_0 values increased for higher ionic strengths. C/C_0 at high ionic strengths became constant approximately in the range of 0.2–0.3. C/C_0 increased when m_f/m_c exceeded 1. This trend was also confirmed in the images shown in Figure 6. The cement removal ability of PGAF was confirmed at all the ionic strengths employed in this experiment. It should be noted that the cement removal by PGAF was limited at high ionic strengths. Figure 5b shows the variations in the pH and EC as a function of the flocculant dose per cement mass m_f/m_c at $I_C = 5.4$ mM. The pH was approximately 11 when m_f/m_c was below 0.1 and sharply dropped to lower than 8 when m_f/m_c was 1. On the other hand, EC tended to decrease very slowly until m_f/m_c reached 1, but began to increase rapidly when m_f/m_c exceeded 1.
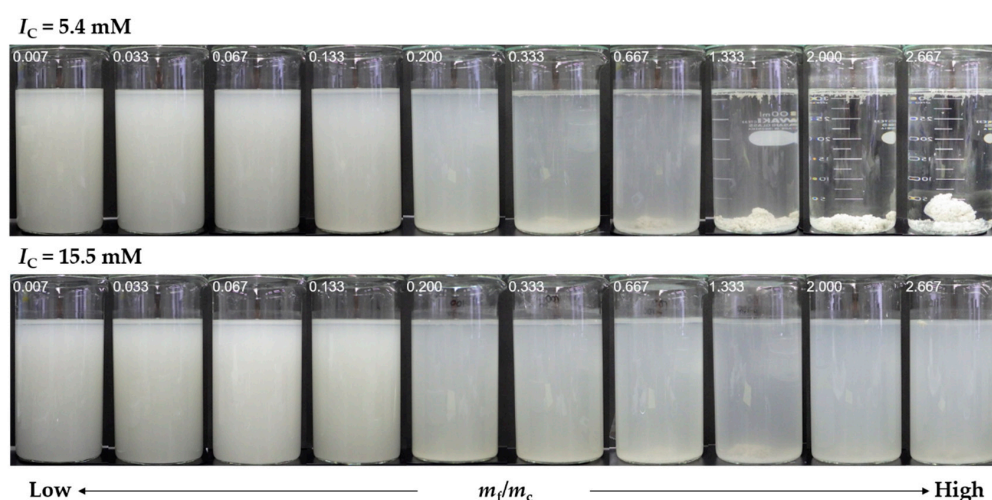

Figure 6. Images of sedimentation state after 30 min. The upper images show the results when the I_C = 5.4 mM, and the lower ones show the results when the I_C = 15.5 mM. The numbers in the images indicate the m_f/m_c. At I_C = 15.5 mM, the turbidity increased with the increase in the addition amount.

3.3. Zeta Potential

Figure 7a shows the zeta potential of the UFC and PGAF as a function of the ionic strength. The zeta potential of the "UFC" was low, i.e., in the range of −10.5 to +5.7 mV within the measured ionic strength. As the ionic strength increased, the zeta potential magnitude of the UFC decreased, changing from negative to positive at 22 mM. The zeta potential of "UFC with SP" was low, i.e., in the range of −12.7 to −2.8 mV, which was slightly greater than that of the UFC without the SP. This shift in the zeta potential was probably due to the adsorption of the SP with carboxyl groups. The zeta potential of the PGAF was positive and ranged from +9 to +25 mV in the range of measured ionic strength. Tsujimoto et al. [32] studied the binding strength of γ-PGA–Ca complex in water, and suggested that the complex globular conformation was owing to the specific interaction between γ-PGA and Ca^{2+}. The PGAF has a large amount of carboxyl groups in cross-linked γ-PGA, for which PGAF takes calcium ions into the cross-linked products, and the resulting complex becomes positive. The mineral particles, calcium sulfate, and calcium carbonate hydrate contained in the PGAF product may have also contributed to the positive zeta potential. The zeta potential saturated over 24 mM probably because of the upper limit of the adsorption capacity of γ-PGA.

Figure 7b shows the zeta potential of the particles in the supernatant of the suspension containing UFC, SP, and PGAF as a function of m_f/m_c for different ionic strengths. The particles of the UFC–PGAF complex in the supernatant water gradually became positively charged. This trend was due to the increase in the ionic strength and the amount of PGAF dose, as deduced from Figure 7a. As for the difference in the potential between $I_C = 5.4$–10 mM and $I_C = 15.5$–44.5 mM after flocculation, we believe the coagulation–flocculation process induced by PGAF changed because of the difference in the ionic strength.
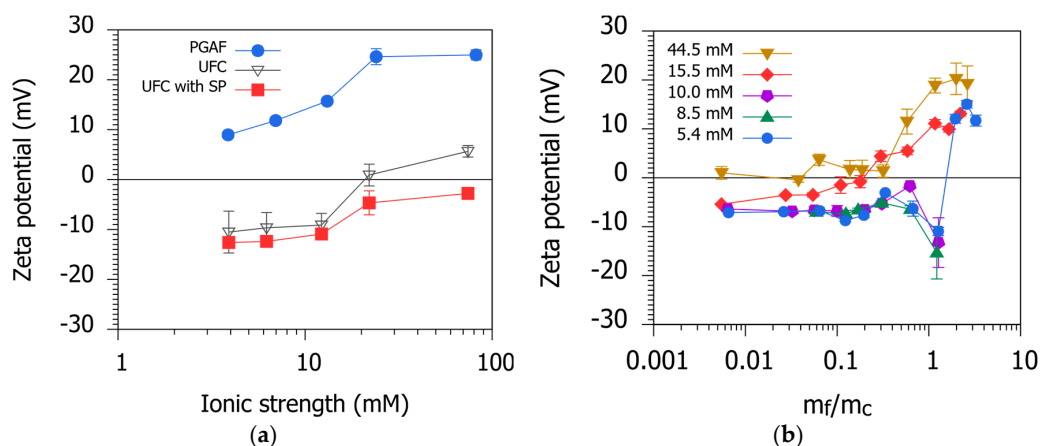
Figure 7. Zeta potential calculated by Smoluchowski's expression: (**a**) zeta potential of PGAF and UFC with SP at each ionic strength; (**b**) zeta potential of particles in the supernatant of UFC with SP and PGAF after 2 h settling against the m_f/m_c.

3.4. Influence of Ionic Strength on Flocculation–Sedimentation Characteristics of PGAF

Figure 8 shows the comparison of the flocs taken from the upper part of the tall beaker after rapid mixing at different ionic strengths. The flocs formed at low ionic strengths, shown in Figure 8a, were larger than the flocs formed at high ionic strengths, shown in Figure 8b. Figure 9 shows the comparison of the particle size distribution and shape of the flocs taken from the supernatant after 30 min settling in the jar test. The median of circularity and aspect ratio were measured as an index of the floc shape [33]. The number of measured samples was 492,418 when I_C = 5.4 mM and 329,974 when I_C = 15.5 mM, respectively.
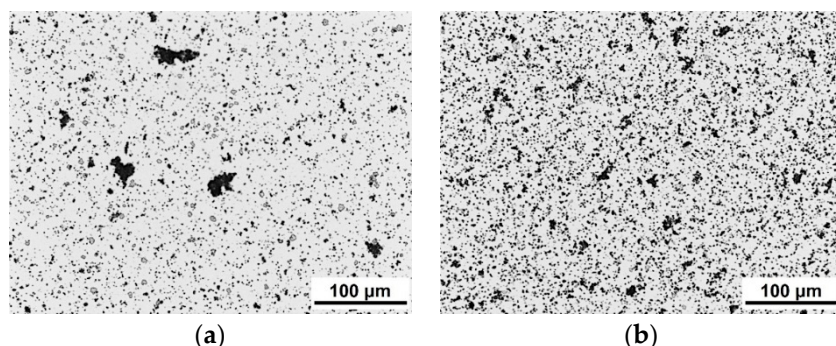

Figure 8. Flocs formed in the upper part at the end of rapid mixing: (**a**) I_C = 5.4 mM, m_f/m_c = 0.2; (**b**) I_C = 15.5 mM, m_f/m_c = 0.2.

$$HS\ Circularity = \frac{4\pi A}{\ell^2}$$

$$Aspect\ ratio = \frac{W}{L}$$

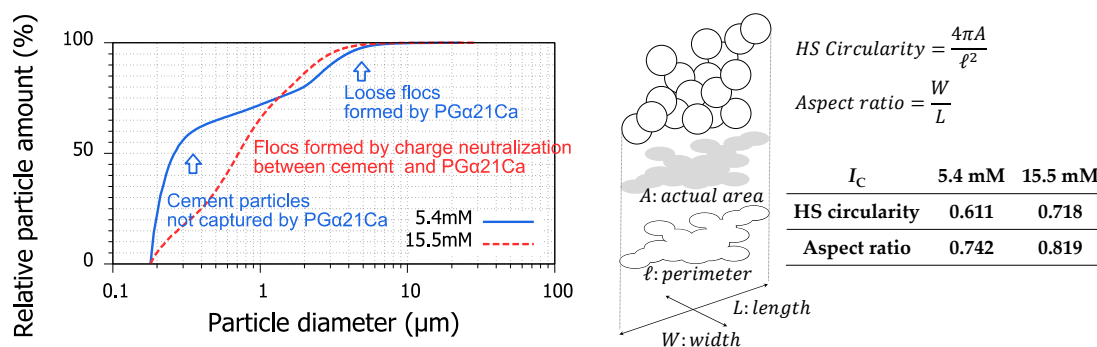| I_C	5.4 mM	15.5 mM
HS circularity	0.611	0.718
Aspect ratio	0.742	0.819

Figure 9. Comparison of particle size distribution and shape of flocs between I_C = 5.4 mM and I_C = 15.5 mM. Each sample was collected from the supernatant after sedimentation of 30 min in the jar test.

The flocs formed at high ionic strengths were more spherical than those formed at low ionic strengths, as indicted by the higher circularity and aspect ratio. On the other hand, the flocs formed at low ionic strengths had an oval shape and appear to have binary peaks in the particle size distribution. Based on this bimodal distribution, the small side peak indicated cement particles that remained suspended without being captured by the PGAF of insufficient amount, whereas the large side peak indicated loose flocs formed by PGAF. In other words, the sweep flocculation induced by PGAF was dominant at low ionic strengths, whereas charge neutralization was the dominant flocculation mechanism at high ionic strengths. From these discussions, we theorized the flocculation process of cement particles induced by PGAF, as shown in Figure 10.
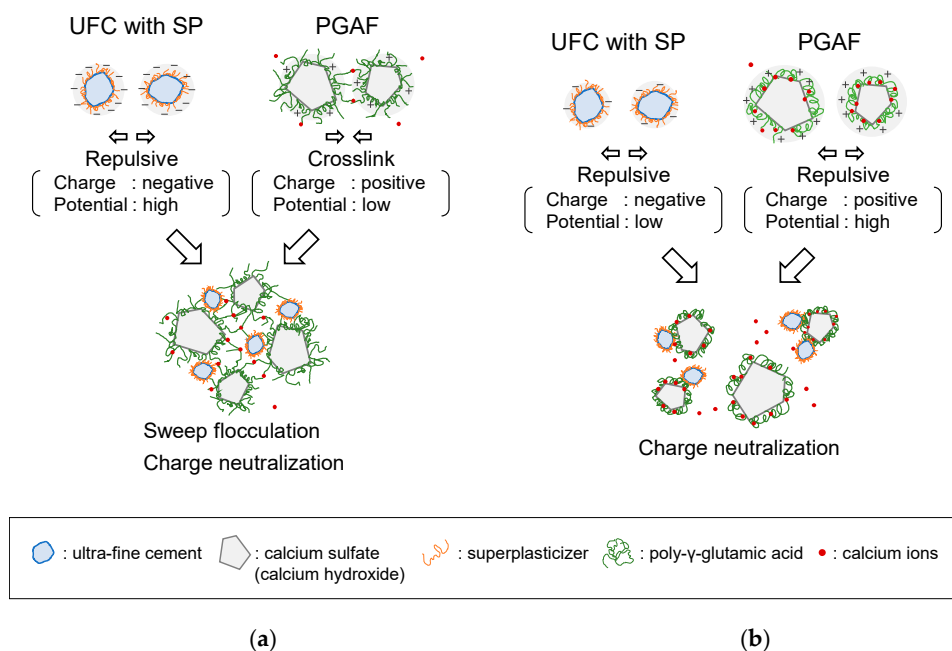

Figure 10. Schematics of the flocculation mechanism of PGAF for cement suspension at: (**a**) low ionic strengths; (**b**) high ionic strengths.

At low ionic strengths, the UFC particles were negatively charged and dispersed by the SP. On the other hand, the PGAF was positively charged. As the calcium ion adsorption did not reach saturation, γ-PGAs bridged between the PGAF particles through the calcium ions [6,34], thus inducing sweep flocculation and charge neutralization, as shown in Figure 10a.

At high ionic strengths, the UFC was negatively and weakly charged, whereas the PGAF exhibited a high positive charge. As the zeta potential of the PGAF reached the upper limit, as shown in Figure 9a, the adsorption amount of the calcium ions could be considered saturated. As such, there was no bridging between the PGAF particles, and therefore, the UFC–PGAF coagulation was due to charge neutralization.

Based on Figure 10, the results of the jar test are explained as follows.

As shown in the data of C/C_0 in Figure 5, the removal effect at high ionic strengths was higher than that at low ionic strengths until m_f/m_c reached 0.1 and when m_f/m_c just exceeded 0.1. The flocs formed by sweep flocculation had a larger particle size but were loose and cloud-like. On the other hand, the flocs formed by charge neutralization were spherical and dense, although the particles were small. Therefore, when m_f/m_c was low, the settling velocity of the flocs formed at high ionic strengths was higher than that of the flocs formed at low ionic strengths.

In Figure 7b, when m_f/m_c was further increased at $I_C = 5.4$ mM, the zeta potential was reversed from -10 to $+15$ mV. This showed that the removal performance was maximum when m_f/m_c reached 1. In Figure 5a, as C/C_0 at this point was still 0.02 or less, the removal efficiency was 98% or more. We believe that the suspended substances remaining in the upper part of the beaker were over-dosed PGAF

particles [35]. They were not entrapped in the UFC–PGAF flocs, but formed PGAF flocs themselves, because sweep flocculation was predominant at low ionic strengths. This led to a high removal ratio.

3.5. Effect of Mixing Intensity

Figures 11 and 12 show the results of increasing the intensity during rapid mixing at 240 rpm for 5 min. These figures show that C/C_0 at 240 rpm was lower than that at 150 rpm when m_f/m_c ranged from 0.03 to 1. In other words, the removal of the UFC particles by PGAF could be improved by increasing the mixing intensity during rapid mixing. The improvement in PGAF removal by increasing the mixing intensity was also confirmed by Ogata et al. [5] for the removal of phosphate ions and by Pan et al. [7] for the removal of kaolin suspension. The results of these experiments were obtained in a system where the ionic strength was not controlled at pH = 5–7; thus, the densification of the formed flocs can be promoted [36]. The results (Figure 11) show that a higher mixing intensity during rapid mixing can improve the removal efficiency of the cement particles by PGAF even under high pH conditions and high ionic strengths.
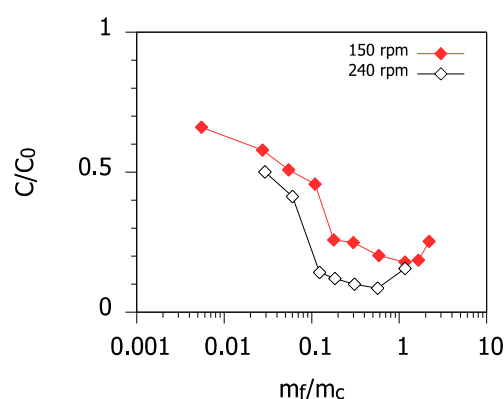

Figure 11. Variation in the C/C_0 with respect to the m_f/m_c in the comparison between rapid mixing at 150 rpm for 3 min and at 240 rpm for 5 min, I_C = 15.5 mM.
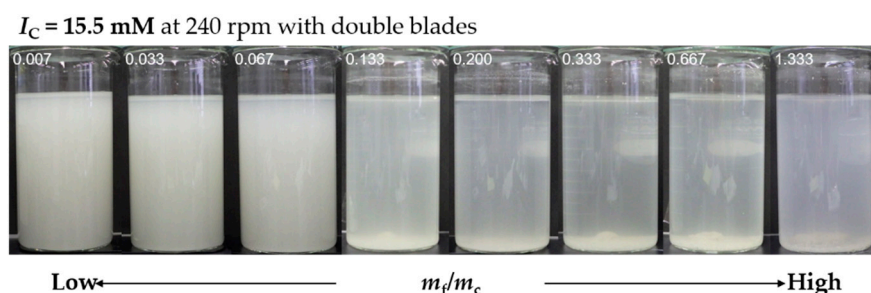

Figure 12. Images of sedimentation state after 30 min. This was a result of rapid mixing at 240 rpm for 5 min with the double blade. The numbers in the images indicate m_f/m_c values. When m_f/m_c was above 1, the turbidity increased again.

As shown in Figure 10b, once the PGAF was exposed to a high ionic strength solution, charge neutralization occurred between the positive shrunken gel-like particles of PGAF and the negative cement particles. In general, a rapid mixing was performed to promote the homogenized mixture of suspended particles and flocculants, and a slow mixing promotes the growth of flocs. The increase in the mixing intensity during rapid mixing also promoted the densification of the micro-flocs formed by charge neutralization at high ionic strengths.

The re-increase tendency of C/C_0 when m_f/m_c was above 1, as shown in Figure 11, was due to flocculant overdosing. The increased EC (Figure 5b) indicated that the minerals contained in PGAF released ions in the solution. When m_f/m_c exceeded 1, an excess PGAF dose per cement particle mass led to an increase in the ionic strength, and the ion uptake into the γ-PGA chain was saturated.

The suspended particles in the upper part of the beaker could be regarded as PGAF particles that could not contribute to charge neutralization and form flocs themselves.

Furthermore, the start of the re-increase at 240 rpm shifted to lower m_f/m_c values compared with that at 150 rpm. This was because increasing the mixing intensity promoted the collision frequency between the PGAF and the UFC with SP particles. This increased the attachment probability of the UFC with respect to the shrunken gel-like particles of the PGAF, and the adsorption amount saturated earlier.

3.6. Applicability of PGα21Ca to Cement Suspension

The removal ratios (%) calculated using $(1 - C/C_0) \times 100$ based on Figure 5a are plotted in the xyz space, as shown in Figure 13a. This figure also shows the x–y plane at 80% as the target removal ratio. Figure 13b shows a diagram connecting the points where m_f/m_c becomes minimum in the x–y plane of each target removal ratio shown in Figure 13a. From this figure, we could determine the optimal addition amount of the flocculant for achieving the target removal rate for cement suspension under any ionic strength. We could use this diagram as a control chart for the flocculation–sedimentation treatment in practice. From this figure and previous discussions, at high ionic strengths, it was particularly important to control the PGAF dose for an appropriate treatment on site. Managing the EC, which is highly correlated with the ionic strength, is considered a useful method to decide optimal dosages.

The results of the laboratory tests and the procedure for obtaining the control charts presented in this study can serve as a basis for an appropriate operation management in practice as well as in a real-time process control [37].
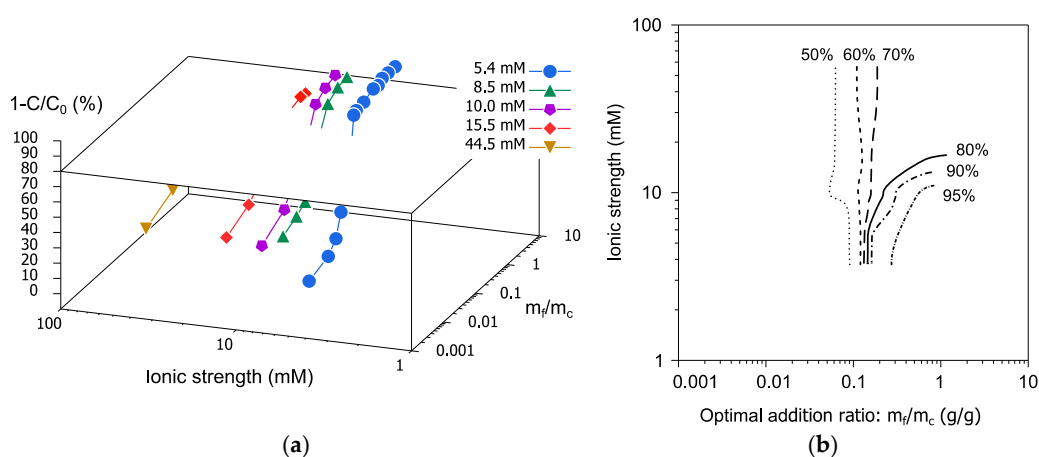

Figure 13. (**a**) Three-dimensional plot of Figure 5a at a removal rate of 80%; (**b**) control chart of optimal addition ratio for each target removal rate.

4. Conclusions

We examined the effect of PGAF on the removal of UFC particles stabilized by a poly-carboxylate co-polymer, which is a SP. We conducted a flocculation–sedimentation treatment with PGAF on a cement suspension under controlled ionic strength and concentration. The removal mechanism and the applicability of this flocculant to cement suspension was investigated in terms of the charge characteristics of the particles.

Following are the results of this study:

- The flocculation–sedimentation treatment with PGAF successfully removed the SP-stabilized UFC particles through the gravitational settling of the formed flocs. However, the removal characteristics at ionic strengths of 10 and 15.5 mM were different.
- From the measurement of the zeta potential, the SP-stabilized UFC was found to be negatively charged. On the other hand, the PGAF was positively charged despite the presence of γ-PGA with carboxyl groups.

- The removal efficiency reduced with the increase in the ionic strength. This decreased removal could have been due to the shrunk form of γ-PGA at high ionic strengths.
- Increasing the mixing intensity during rapid mixing improved the removal efficiency even at high ionic strengths.
- Based on a series of flocculation–sedimentation experiments, the removal ratios against ionic strengths and m_f/m_c was plotted in the three-dimensional diagram.
- Using this diagram as a control chart, we can determine the optimal addition amount of the PGAF for achieving the target removal rate for cement suspension under any ionic strengths.

PGAF was found to be a good candidate for the purification of cement suspensions by flocculation–sedimentation, and a better removal performance could be obtained at lower ionic strengths with intense rapid mixing. The results of the laboratory tests and the procedure for obtaining the control charts presented in this study can serve as a basis for an appropriate operation management in practice as well as in the design stage. In on-site practice, managing the EC, which is highly correlated with the ionic strength, is considered a useful method to decide optimal dosages. In the design stage, when a desired removal rate cannot be obtained only by the flocculation–sedimentation treatment, an integration with the other treatment is considered [38,39]. The results of this test can be used as an effective indicator for flocculation–sedimentation treatments and in designs that integrate filtration operation.

Author Contributions: T.Y. conceived the idea and methodology for the project and conducted experiments, as well as wrote the draft of this paper. M.K. conceived the idea for the project and provided ideas for the analysis of the results, as well as supervised the research and checked and improved this paper. K.O. conducted the concentration measurement and analysis by ion chromatography and confirmed the validity of the results and checked this paper.

Conflicts of Interest: The authors declare no conflicts of interest.

Abbreviations

Abbreviation	Description
PGAF	poly-γ-glutamic acid flocculant
UFC	ultra-fine cement
SP	superplasticizer
γ-PGA	poly-γ-glutamic acid
PAC	poly-aluminum chloride
BFSC	blast furnace slag cement
OPC	ordinary Portland cement
AE	air-entrainment
EC	electrical conductivity
I_C	ionic strength of cement suspension
C	absorbance of supernatant after flocculation–sedimentation
C_0	initial absorbance of cement suspension
C/C_0	the ratio of the absorbance of the supernatant to that of the initial suspension
w/c	water-to-cement mass ratio
m_f	mass of PGAF
m_c	mass of UFC
m_f/m_c	PGAF-to-UFC mass ratio

References

1.　Ridi, F.; Fratini, E.; Baglioni, P. Cement: A two thousand year old nano-colloid. *J. Colloid Interface Sci.* **2011**, *357*, 255–264. [CrossRef] [PubMed]

2.　Amirtharajah, A.; Mills, K.M. Rapid-mix design for mechanisms of alum coagulation. *J. AWWA* **1982**, *74*, 210–216. [CrossRef]

3.　Bhatti, Z.A.; Mahmood, Q.; Raja, I.A. Sewage water pollutants removal efficiency correlates to the concentration gradient of amendments. *J. Chem. Soc. Pak.* **2009**, *31*, 665–673.

4.　de Paula, H.M.; de Oliveira Ilha, M.S.; Andrade, L.S. Concrete plant wastewater treatment process by coagulation combining aluminum sulfate and *Moringa oleifera* powder. *J. Clean. Prod.* **2014**, *76*, 125–130. [CrossRef]

5.　Ogata, F.; Ueda, A.; Kawasaki, N. Removal of phosphate ions by PGAF (poly-γ-glutamic acid and flocculants). *J. Water Environ. Technol.* **2014**, *12*, 447–458. [CrossRef]

6.　Bajaj, I.B.; Singhal, R.S. Flocculation properties of poly (γ-glutamic acid) produced from *Bacillus subtilis* isolate. *Food Bioprocess Technol.* **2011**, *4*, 745–752. [CrossRef]

7.　Pan, Y.; Shi, B.; Zhang, Y. Research on flocculation property of bioflocculant PG·a21 Ca. *Mod. Appl. Sci.* **2009**, *3*, 106–112. [CrossRef]

8.　Taniguchi, M.; Kato, K.; Matsui, O.; Ping, X.; Nakayama, H.; Usuki, Y.; Ichimura, A.; Fujita, K.; Tanaka, T.; Tarui, Y.; et al. Flocculating activity of cross-linked poly-γ-glutamic acid against bentonite and *Escherichia coli* suspension pretreated with $FeCl_3$ and its interaction with Fe^{3+}. *J. Biosci. Bioeng.* **2005**, *100*, 207–211. [CrossRef]

9.　Yokoi, H.; Arima, T.; Hirose, J.; Hayashi, S.; Takasaki, Y. Flocculation properties of poly (γ-glutamic acid) produced by *Bacillus subtilis*. *J. Ferment. Bioeng.* **1996**, *82*, 84–87. [CrossRef]

10.　Campos, V.; Fernandes, A.R.A.C.; Medeiros, T.A.M.; Andrade, E.L. Physicochemical characterization and evaluation of PGA bioflocculant in coagulation-flocculation and sedimentation processes. *J. Environ. Chem. Eng.* **2016**, *4*, 3753–3760. [CrossRef]

11.　Carvajal-Zarrabal, O.; Nolasco-Hipólito, C.; Barradas-Dermitz, D.M.; Hayward-Jones, P.M.; Aguilar-Uscanga, M.G.; Bujang, K. Treatment of vinasse from tequila production using polyglutamic acid. *J. Environ. Manag.* **2012**, *95*, S66–S70. [CrossRef] [PubMed]

12.　Kobayashi, M.; Nitanai, M.; Satta, N.; Adachi, Y. Coagulation and charging of latex particles in the presence of imogolite. *Colloids Surf. A Physicochem. Eng. Asp.* **2013**, *435*, 139–146. [CrossRef]

13.　Uchikawa, H.; Hanehara, S.; Sawaki, D. The role of steric repulsive force in the dispersion of cement particles in fresh paste prepared with organic admixture. *Cem. Concr. Res.* **1997**, *27*, 37–50. [CrossRef]

14.　Plank, J.; Pöllmann, K.; Zouaoui, N.; Andres, P.R.; Schaefer, C. Synthesis and performance of methacrylic ester based polycarboxylate superplasticizers possessing hydroxy terminated poly (ethylene glycol) side chains. *Cem. Concr. Res.* **2008**, *38*, 1210–1216. [CrossRef]

15.　Zhang, Y.; Kong, X. Correlations of the dispersing capability of NSF and PCE types of superplasticizer and their impacts on cement hydration with the adsorption in fresh cement pastes. *Cem. Concr. Res.* **2015**, *69*, 1–9. [CrossRef]

16.　Hirata, T.; Ye, J.; Branicio, P.; Zheng, J.; Lange, A.; Plank, J.; Sullivan, M. Adsorbed conformations of PCE superplasticizers in cement pore solution unraveled by molecular dynamics simulations. *Sci. Rep.* **2017**, *7*, 1–10. [CrossRef] [PubMed]

17.　Silsbee, M.; Malek, R.I.A.; Roy, D.M. Composition of pore fluids extruded from slag-cement pastes. In Proceedings of the 8th International Congress on the Chemistry of Cement, Rio de Janeiro, Brazil, 22–27 September 1986; Volume IV, pp. 263–269.

18.　Andersson, K.; Allard, B.; Bengtsson, M.; Magnusson, B. Chemical composition of cement pore solutions. *Cem. Concr. Res.* **1989**, *19*, 327–332. [CrossRef]

19.　Neubauer, C.M.; Yang, M.; Jennings, H.M. Interparticle potential and sedimentation behavior of cement suspensions: Effects of admixtures. *Adv. Cem. Based Mater.* **1998**, *8*, 17–27. [CrossRef]

20.　Lowke, D.; Gehlen, C. The zeta potential of cement and additions in cementitious suspensions with high solid fraction. *Cem. Concr. Res.* **2017**, *95*, 195–204. [CrossRef]

21.　Yang, M.; Neubauer, C.M.; Jennings, H.M. Interparticle potential and sedimentation behavior of cement suspensions review and results from paste. *Adv. Cem. Based Mater.* **1997**, *5*, 1–7. [CrossRef]

22. Kobayashi, M.; Adachi, Y.; Ooi, S. Breakup of fractal flocs in a turbulent flow. *Langmuir* **2002**, *15*, 4351–4356. [CrossRef]
23. Sugimoto, T.; Nishiya, M.; Kobayashi, M. Charge reversal of sulfate latex particles in the presence of lanthanum ion. *Colloids Surf. A Physicochem. Eng. Asp.* **2019**, *572*, 18–26. [CrossRef]
24. Takeshita, C.; Masuda, K.; Kobayashi, M. The effect of monovalent anion species on the aggregation and charging of allophane clay nanoparticles. *Colloids Surf. A Physicochem. Eng. Asp.* **2019**, *577*, 103–109. [CrossRef]
25. Viallis-Terrisse, H.; Nonat, A.; Petit, J.C. Zeta-potential study of calcium silicate hydrates interacting with alkaline cations. *J. Colloid Interface Sci.* **2001**, *244*, 58–65. [CrossRef]
26. Pointeau, I.; Reiller, P.; Macé, N.; Landesman, C.; Coreau, N. Measurement and modeling of the surface potential evolution of hydrated cement pastes as a function of degradation. *J. Colloid Interface Sci.* **2006**, *300*, 33–44. [CrossRef] [PubMed]
27. Lowke, D.; Gehlen, C. The effect of pore solution composition on zeta potential and superplasticizer adsorption. In Proceedings of the 11th International Conference on Superplasticizers and Other Chemical Admixtures in Concrete, Ottawa, ON, Canada, 10–13 July 2015; pp. 253–264.
28. Plank, J.; Hirsch, C. Impact of zeta potential of early cement hydration phases on superplasticizer adsorption. *Cem. Concr. Res.* **2007**, *37*, 537–542. [CrossRef]
29. Zingg, A.; Winnefeld, F.; Holzer, L.; Pakusch, J.; Becker, S.; Gauckler, L. Adsorption of polyelectrolytes and its influence on the rheology, zeta potential, and microstructure of various cement and hydrate phases. *J. Colloid Interface Sci.* **2008**, *323*, 301–312. [CrossRef] [PubMed]
30. Ferrari, L.; Kaufmann, J.; Winnefeld, F.; Plank, J. Interaction of cement model systems with superplasticizers investigated by atomic force microscopy, zeta potential, and adsorption measurements. *J. Colloid Interface Sci.* **2010**, *347*, 15–24. [CrossRef] [PubMed]
31. Tian, H.; Kong, X.; Su, T.; Wang, D. Comparative study of two PCE superplasticizers with varied charge density in Portland cement and sulfoaluminate cement systems. *Cem. Concr. Res.* **2019**, *115*, 43–58. [CrossRef]
32. Tsujimoto, T.; Kimura, J.; Takeuchi, Y.; Uyama, H.; Park, C.; Sung, M.H. Chelation of calcium ions by poly (γ-glutamic acid) from bacillus subtilis. *J. Microbiol. Biotechnol.* **2010**, *20*, 1436–1439. [CrossRef]
33. Ulusoy, U.; Kursun, I. Comparison of different 2D image analysis measurement techniques for the shape of talc particles produced by different media milling. *Miner. Eng.* **2011**, *24*, 91–97. [CrossRef]
34. Nap, R.J.; Szleifer, I. Effect of calcium ions on the interactions between surfaces end-grafted with weak polyelectrolytes. *J. Chem. Phys.* **2018**, *149*, 163309. [CrossRef] [PubMed]
35. Szilagyi, I.; Trefalt, G.; Tiraferri, A.; Maroni, P.; Borkovec, M. Polyelectrolyte adsorption, interparticle forces, and colloidal aggregation. *Soft Matter* **2014**, *10*, 2479–2502. [CrossRef] [PubMed]
36. Adachi, Y.; Kobayashi, A.; Kobayashi, M. Structure of colloidal flocs in relation to the dynamic properties of unstable suspension. *Int. J. Polym. Sci.* **2012**, *2012*, 1–14. [CrossRef]
37. Ratnaweera, H.; Fettig, J. State of the art of online monitoring and control of the coagulation process. *Water* **2015**, *7*, 6574–6597. [CrossRef]
38. Hägg, K.; Cimbritz, M.; Persson, K.M. Combining chemical flocculation and disc filtration with managed aquifer recharge. *Water* **2018**, *10*, 1854. [CrossRef]
39. Bu, F.; Gao, B.; Yue, Q.; Liu, C.; Wang, W.; Shen, X. The combination of coagulation and adsorption for controlling ultra-filtration membrane fouling in water treatment. *Water* **2019**, *11*, 90. [CrossRef]